Design of Hydrofoil Assisted Catamarans using a Non-Linear Vortex Lattice Method

Nikolai Kornev[2]; Günther Migeotte[1]; Karl Günter Hoppe[3]; Anna Nesterova[4]
[1, 3] Dept. of Mechanical Engineering, University of Stellenbosch: migeotte@ing.sun.ac.za
[2, 4] Marine Technical University of St. Petersburg: kornev@spb.cityline.ru

Abstract
Extensive experimental investigations of hydrofoil-assisted catamarans have identified the main hydrodynamic parameters affecting the performance of these vessels. Design principles of existing vessels are discussed in the light of these hydrodynamic findings. The experience gained from experimental testing has provided the basis for the development of a non-linear vortex lattice method for design purposes. The method is validated by comparison with experimental results and applied to the problem of optimizing a 40-knot, 40m hydrofoil-assisted catamaran with a hydrofoil system developed for modern high-speed catamarans. It is shown that the method can be successfully applied to optimization problems of these vessels as it successfully captures the complex hull-foil interactions. Results of the numerical investigation performed, indicate that optimizing the mutual distance between the hydrofoils can significantly improve the lift to drag ratio of such a vessel.

1. Introduction

The development of hydrofoil assisted catamarans started in the late 70's with developments in the Soviet Union and in the early 80's with developments in the USA and South Africa. Early developments focused on the design of smaller planing type catamarans with asymmetric hulls using up to three foils mounted in tandem between the demi-hulls. Over the last decade, the application of hydrofoil assistance has extended to include the more modern high-speed semi-displacement type catamarans used mainly for fast ferry applications. While the application of small hydrofoils for these vessels is well known and popular for sea-keeping improvements, the use of larger hydrofoils for improvements in resistance is less well known and is the focus of this paper.

Since the early 80's, the University of Stellenbosch has been involved with development of hydrofoil-assisted catamarans of sizes ranging from 5m to 40m. A practical and successful foil system was patented and named "Hysucat," Hoppe (1982). Hysucats were developed through systematical towing tank tests and planing craft theory. Later a mathematical model was developed using Savitsky's (1964) formulations and hydrofoil theory as applied to hydrofoil craft, Hoppe (1991, 1995). Good results were achieved and later Hysucats were designed and optimized by use of the mathematical model alone without the need for model tests. The experience built up in the design of Hysucats has more recently applied to catamarans with semi-displacement hull forms. A new, patented foil system named "Hysuwac", Hoppe (1998), was specifically developed for larger semi-displacement type catamarans. Application of Hysuwac and other foil systems to semi-displacement type catamarans is still relatively new, with only a hand full of vessels that have been built worldwide. This paper describes some of the hydrodynamic design aspects of hydrofoils for modern high-speed catamarans based on experimental results, prototype data and numerical calculations carried out on Hysuwac and other hydrofoil configurations.

2. Hydrodynamic Principles

A hydrofoil-assisted catamaran achieves superior performance over a conventional catamaran by

unloading the hull and lifting it partially out of the water. This has two major influences on resistance: reduced friction resistance due to a decreased wetted area and secondly, reduced hull wave making. In addition to the positive effects introduced by the foil assistance, one has to consider the added resistance of the foils and the interference resistance coming from hull-foil and foil-foil interactions. Figure 1 shows a resistance breakdown for a hydrofoil-assisted catamaran. The figure attempts to breakdown the resistance components into their well-known parts and indicate how the different components interact with each other. A detailed explanation of these is given in Migeotte and Hoppe (1999).

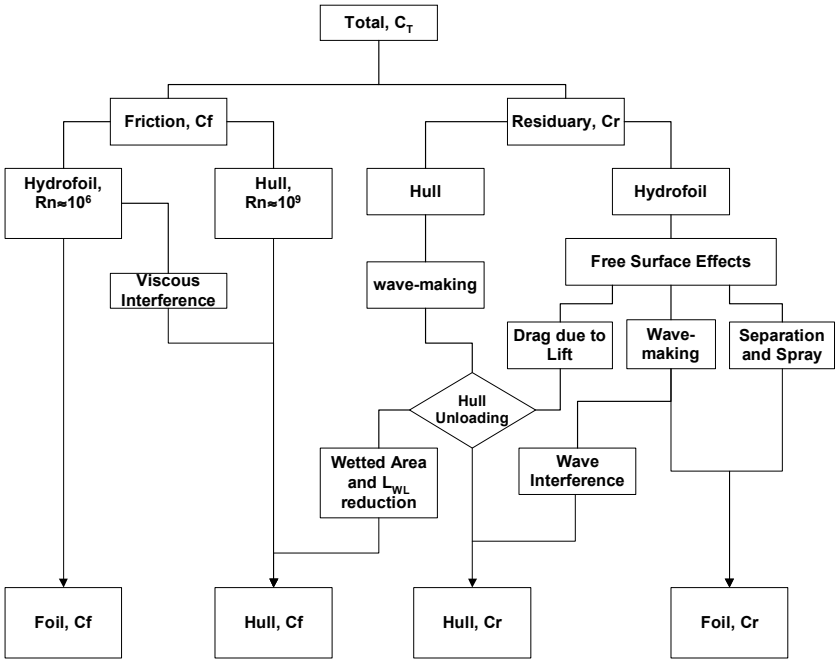

Figure 1: Resistance Components for Hydrofoil Assisted Vessels

Due to the hull being constantly unloaded with increasing speed, determining the resistance components is not an easy task. The *foil* resistance components are the easiest to calculate, as foil theory is well developed. There is some measure of uncertainty in all calculations due to hull-foil interference effects. These are mainly wave-making interference, disturbed inflow conditions to the foils and the 'end-plate' effect of the hull on the foils. Hoerner (1965) and Tao (2000) give some equations on how to estimate these empirically. Alternatively, one can apply CFD methods to determine these effects.

Determining the *hull* resistance components is difficult without the use of model tests. An important point to note is that the hull of a foil-assisted catamaran differs from a conventional catamaran hull, in that being constantly unloaded, it has no fixed displacement, so one is not able to rely on catamaran model test databases to predict performance. Unloading the hull by effects the two most important parameters governing hull resistance:

- The *hull* length displacement ratio, $L/\nabla^{1/3}$, where ∇ is the volumetric displacement of the submerged part of the hull.
- The *hull* Froude displacement number, Fn_∇, again based on the load fraction of the hull.

Values of both parameters are higher for the hulls alone than that for the complete vessel. More often than not, this means that the available experimental results for high-speed catamarans is not applicable as either of these two parameters falls out of the range of data. The foils additionally

have a significant effect on the pressure of the hull. Depending on the foil configuration these effects may be positive or negative. If the hull is in close proximity to the suction side of the foil, (for example a foil located slightly below the keel) the hull will suffer from the foil's downwash and pressures will be lower than normal in that area. The inverse obviously also applies: the foil can be positioned so that the hull benefits from the up wash of the foils. A typical example is a foil mounted in the tunnel between the demi-hulls. The vortex wake of the foil will induce up wash on the sections of the hull aft of the foil. Such dynamic effects can have important influence on the behavior and resistance of the vessel.

Analysis of the large body of experimental data collected on hydrofoil-assisted catamarans at the University of Stellenbosch has allowed certain tendencies to be established that have proven useful in the design process. Hydrodynamically, one can identify three phases of operation of hydrofoil-assisted catamarans (Figure 2): the displacement/semi-displacement phase, the transition from semi-displacement to planing and finally the planing phase.

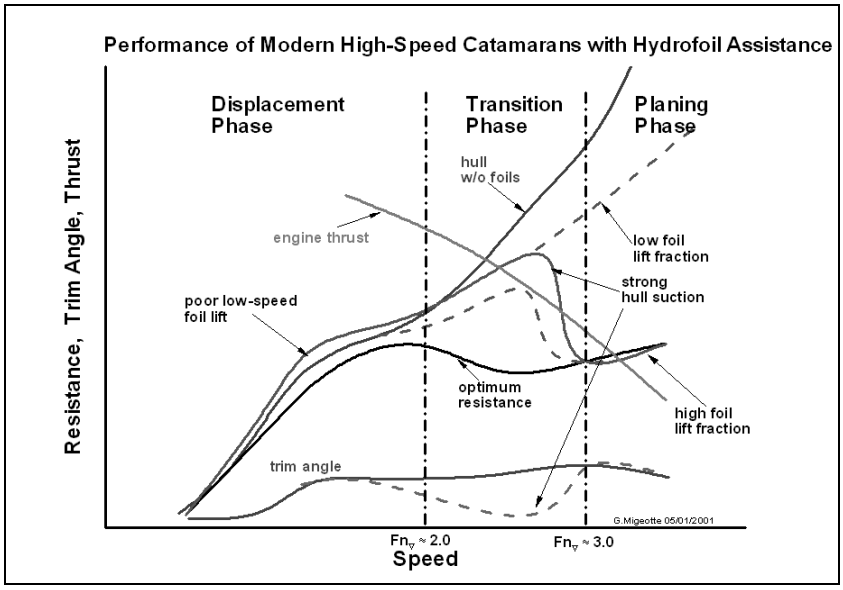

Figure 2: Hydrodynamic Phases of hydrofoil Assisted Catamarans

At present hydrofoil-assistance does not make sense for vessels operating below the displacement hump ($Fn_\nabla \approx 1.5$). Since the weight of a craft is proportional to the cube of a linear dimension and the lift to the square of the linear dimension, the required size for a foil system out grows practical sizes for these speeds. To the knowledge of the authors, $Fn_\nabla = 1.5$ is currently the lower limit for which hydrofoil assistance has been designed to provide a useful improvement in resistance (Hoppe and Migeotte (2000)).

The transition phase (approx. $2.0<Fn_\nabla<3.0$) is the most complex hydrodynamically. The increasingly dominant hydrodynamic forces (as opposed to hydrostatic forces dominating at lower speeds) acting on the hull cause the hull to suck itself down, opposing the foil lift. It is common for non-foil-assisted high-speed catamarans to submerge slightly with speed, as the hydrodynamic suction forces on the hull increase. The sudden disappearance of these suction forces on the hull signifying the beginning of true planing are the cause of the large and sudden reductions in resistance in the transition phase. Existing hydrofoil assisted catamarans (a review of existing vessels is given in Migeotte and Hoppe (1999) and Hoppe (1991, 1995, 1999) operating in this range try and avoid these sudden changes due to suction by either making the

hulls very slender (e.g. the Hitachi "Superjet" catamarans, Miyata (1989)) or designing them so that they develop mostly positive dynamic lift (e.g. Kvaerner "FoilCat," Jorde (1991)). Experimental investigation of various foil positions is usually needed to determine the optimal foil design to minimize these effects.

True planing speeds (approx. Fn_∇>3.0) are the easiest to design for, as both hull and foils operate efficiently in this speed range and positive interference effects can more easily be utilized in the design. Simple planing hull lines can be utilized with smaller foils mounted out of harms way in the tunnel between the demi-hulls.

3. Hydrofoil Assisted Catamaran Designs

Examining existing vessels provides some example of the various options that are available. Figure 3 summarizes the established foil configurations currently in use on existing high-speed semi-displacement vessels:

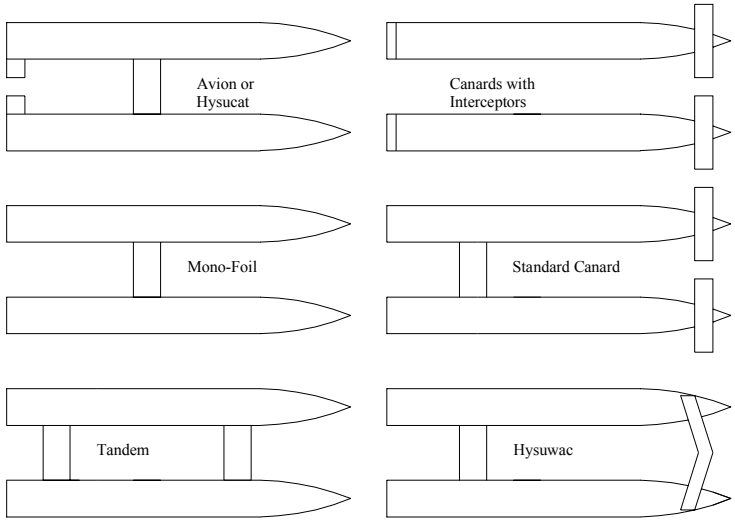

Figure 3: Foil Configurations for Hydrofoil Assisted Catamarans

The tandem and standard canard configurations are the most popular for semi-displacement type craft, the bulk of existing craft making use of these two systems. This is mainly due to their large lifting capability allowing the complete vessel to be lifted out of the water if needed. This makes the system less sensitive to LCG shifts and overloading. The avion system has found application on a large number (200+) of planing catamarans ranging from 5 to 20m but limited application to semi-displacement type vessels (one 36m vessel) due to its limited lift capability at semi-displacement speeds. Similarly, the simpler mono-foil has also only seen one successful application for a 40m semi-displacement type vessel. The canard only system, usually coupled with a transom interceptor, has seen two applications both designed by the patent owners, MTD-St. Petersburg for 30m high-speed planing ferries. The Hysuwac system to date has been applied to three vessels. The Hysuwac system utilizes a high aspect ratio front foil together with a rear foil mounted in the tunnel. The system has been applied to vessels ranging from 20m to 40m and successful designs completed for vessels up to 72m.

One can presently distinguish between two kinds of vessel designs: those of new vessels with hull and foils optimized to match and hydrofoil retrofits to existing catamarans, where foils are matched to an existing hull. The design of new vessels allows the designer more freedom in avoiding potential problems of interference, making the design somewhat simpler if one has

experience in these effects. Positive effects such as wave cancellation and taking advantage of the up wash from the hydrofoils to increase the hull lift can be effectively used to minimize resistance. Utilizing these effects allows one to achieve the resistance tendencies considered optimum as indicated in Figure 2.

Hydrofoil retrofits tend to be more difficult because a hull not designed to be dynamically unloaded risks being unstable in some way (directional stability being the most common problem). Experience with Hysuwac type retrofits to existing hulls has shown that the main difficulty lies in achieving suitable transition phase resistance and behavior. It is also more difficult to take advantage of positive interference effects between hull and foils as the foil design is dictated more by factors such as stability and structural requirements. Hydrofoil retrofits, while not optimal, can nevertheless significantly improve the vessel efficiency and speed. This has been proven on Hysuwac foil retrofits to commercial craft performed by the University of Stellenbosch.

Worldwide, initial development and design of new hydrofoil assisted semi-displacement catamarans has relied heavily on experimental model testing in the design process. Such experiments are invaluable for identifying the main hydrodynamic problems and finding suitable solutions for these. A number of publications, based on experimental investigations, are available that provide some experimental data (see for example (Hoppe (1984), Miyata (1990), Shimizu (1994), Tao (1998, 2000), Migeotte and Hoppe (1999)) useful for design purposes.

From such experimental investigations, enough experience has been built up at the University of Stellenbosch making it possible, with the aid of the CFD knowledge of the Marine Technical University of St. Petersburg, to develop a suitable computational method to aid in the design process and reduce the required towing tank time. As an example of the application and usefulness of the method, the design of Hysuwac hydrofoils for a benchmark size passenger catamaran will be considered. Such a vessel has typical dimensions as given in Table 1. This design was developed by use of the mathematical model for Hysucats, Hoppe (1991, 1995) and systematical towing tank tests at the University of Stellenbosch.

Table 1: Catamaran Main Particulars

Overall Length	40 m
Displacement	170 t
Installed Power	2 x 2200 kW
Speed w/o foils	36 knots
Speed with foils	Approx. 45 knots

Application of the method is described for speeds in the upper end of the transition phase and higher. This covers the design speeds of the vessel with and without foils. This requires one to consider numerical methods that can adequately model semi-planing and planing in combination with hydrofoils. The theoretical method implemented in the commercial package AUTOWING, developed by Dr. Kornev (1998) at the Marine Technical University of St. Petersburg, is particularly suited to for these types of calculations. Combined with the expertise gained from experimental work, the method was further developed for application to hydrofoil-assisted catamarans.

4. Theoretical method

Hydrodynamically, the hydrofoil-assisted catamaran at high speed can be considered as consisting of two parts: the front foil and the aft hull plus rear foil. The parts are considered

separately. The front foil is calculated as a wing moving under the undisturbed free surface. The hydrodynamic effects of the aft hull and rear foil on the front foil are neglected. This has been found to be a valid assumption if the front foil is located forward near the bow. The aft hull and the rear foil are treated as a wing system moving in the vortex-wave wake shed from the front foil.

4.1 Treatment of the free surface problems

To calculate the wave surface and vortex wake after the front hydrofoil, a three-dimensional Nonlinear Vortex Lattice Method (NLVM) was developed. The intensity of the discrete vortices on the free surface is found from the free surface dynamic boundary conditions (both linear and nonlinear) whereas the form of the free surface is sought from the free surface kinematic boundary conditions.

For a short description of the NLVM application to free surface problems, we consider a hydrofoil advancing at constant forward speed V_∞ in an incompressible, inviscid and irrotational fluid. We use a Cartesian coordinate system fixed to the foil; x points forward, y upward and z in transverse direction. The free surface is modeled by a vortex sheet with unknown intensity, $\vec{\gamma}$. Without loss of generality, we can decompose $\vec{\gamma}$ at each point on the free surface within the computational domain as the sum of two components tangential to the free surface: $\vec{\gamma}_\zeta$ is the component perpendicular to the x-axis, $\vec{\gamma}_\xi$ is perpendicular to $\vec{\gamma}_\zeta$. The governing equation for the perpendicular component, $\vec{\gamma}_\zeta$ can be obtained from the dynamic boundary condition (see Kornev and Taranov (1998)):

$$\vec{\bar{\gamma}}_\zeta = \left|\bar{v}_0^2\right| + (\vec{n} \times \vec{\bar{\gamma}})\vec{\bar{v}}_0 + \frac{1}{4}\left|\bar{\gamma}^2\right| + 2\frac{\bar{y}_w}{Fn^2} - 2\bar{v}_{ox} \tag{1}$$

Where, $\bar{\gamma} = \gamma / V_\infty$, $\bar{v}_0 = v_0 / V_\infty$, the wave ordinate $\bar{y}_w = y_w / L$, $Fn = V_\infty / \sqrt{gL}$ are non-dimensionalized with respect to speed of motion, V_∞ and wing chord length, L. The velocity on the free surface, $\vec{v}_0$ induced by the front foil and the vortex sheet $\vec{\gamma}$ can be calculated using Biot-Savart's law. Together with the zero-divergence condition and conditions at infinity,

$$\nabla\vec{\gamma} = 0, \qquad ,|\gamma| \to 0, \qquad for \qquad |z| \to \pm\infty,$$

$$y_w(+\infty, z) = 0, \qquad \gamma(+\infty, z) = 0 \tag{2}$$

(1) represents a complete system of governing equations for the vector intensity, $\vec{\gamma}$.

In the numerical implementation, the free surface is modeled within a rectangle defined by x_0, x_1, z_0 and z_1. As usual in the vortex lattice method, the surface Vorticity $\vec{\gamma}$ is represented by a number of closed vortices (see Fig. 4). Thus, the first equation in Eq. (2) is satisfied automatically in the integral sense. For the panelization of the free surface along the x-axis two procedures were investigated: a procedure proposed by Thiart (1997) and simple exponential stretching

$$x_j = x_{j-1} - \Delta x[1 + N(1 - \exp\{-0.1(x_{j-1} - X)^2\})] \tag{3}$$

where X is the abscissa of the leading edge of the hydrofoil and Δx and N are free parameters. Surprisingly we have obtained almost the same results for both panelizations. In the lateral direction the wave surface is divided into panels uniformly between struts and the simple stretching (3) is used outside of ship's width.

The vector equation (1) is satisfied at the center of each vortex lattice. The vector intensity, $\vec{\gamma}$, necessary for calculations of the RHS of Eq (1) is sought by smoothing the discrete vortices according to simple formula:

$$\vec{\gamma}^{\,m} = [(\Gamma_{ij}^m - \Gamma_{ij-1}^m)\frac{\vec{R}_{00}^m}{|\vec{R}_{00}^m|} + (\Gamma_{ij+1}^m - \Gamma_{ij}^m)\frac{\vec{R}_{11}^m}{|\vec{R}_{11}^m|}]/(|\vec{R}_{01}^m| + |\vec{R}_{10}^m|) +$$

$$[(\Gamma_{i+1j}^m - \Gamma_{ij}^m)\frac{\vec{R}_{10}^m}{|\vec{R}_{10}^m|} + (\Gamma_{ij}^m - \Gamma_{i-1j}^m)\frac{\vec{R}_{01}^m}{|\vec{R}_{01}^m|}]/(|\vec{R}_{00}^m| + |\vec{R}_{11}^m|) \quad (4)$$

Where: Γ_{ij}^m is the strength of ij-th discrete vortex and m is the number of iterations. As soon as the vortex intensity, $\vec{\gamma}^{m+1}$ is found from Eq. (1), the continuous vortex sheet is redistributed among the discrete closed vortices

$$\Gamma_{ij}^{m+1} = \Gamma_{ij-1}^{m+1} + \vec{\gamma}^{m+1}(|\vec{R}_{01}^m| + |\vec{R}_{10}^m|)/2 \quad (5)$$

The kinematic condition on the free surface is used to calculate the shape of the free surface and to adjust the height of the vortex lattice. More precisely the form of the free surface is determined from the solution of the streamline equations

$$\frac{dx}{v_{0x}} = \frac{dy}{v_{oy}} = \frac{dz}{v_{oz}} \quad (6)$$

The velocity at each knot of the vortex lattice are found using the rule (designations see in the Fig.4)

$$\vec{W} = (\vec{V}_{+-} + \vec{V}_{-+} + \vec{V}_{--} + \vec{V}_{++})/4$$

To separate the vectors $\vec{\gamma}_\zeta$ and $\vec{\gamma}_\xi$, as it requires the numerical implementation of the Eq. (1), the vortex lattice on the free surface should satisfy the following conditions:

the lateral sections of every closed vortex lie in the plane x=const, (7a)

the longitudinal sections lie in the plane z=const. (7b)

Certainly after solution of the streamline equations we obtain the lattice violating the condition (7b). Therefore, a special procedure is used to build a necessary orthogonal grid on the base of calculated one at each iteration step. This algorithm works only if the waves do not break. Both $\vec{\gamma}$ and y_w are assumed zero at both side boundaries of the modeled free surface region.

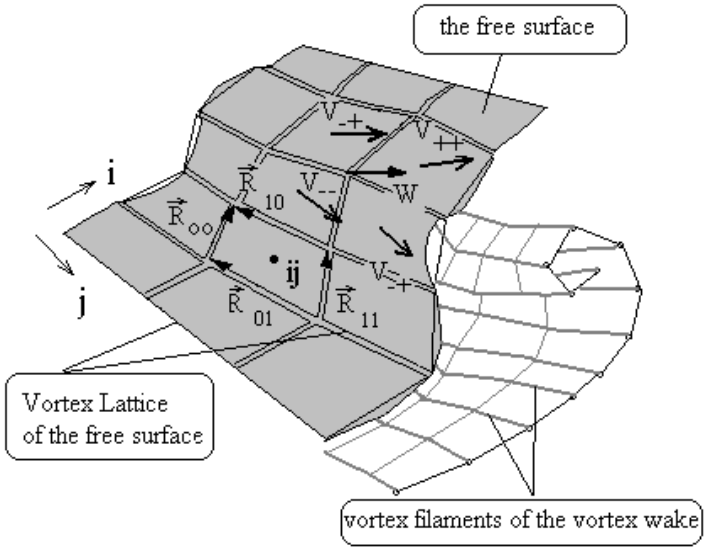

Figure 4: Vortex Lattice of the free surface and vortex wake behind the hydrofoil

4.2 Calculation of the hydrofoil

The hydrofoil and its vortex wake are treated using the common NVLM method described comprehensively in many textbooks and special papers. The numerical instability, which is typical for problems including the dynamics of thin vortex sheets, was avoided using the concept of the cut-off radius. The thickness of hydrofoil is accounted for by a source distribution with strength equal to the thickness gradient in downstream direction.
The calculation of the hydrofoil under the free surface is performed using a special iterative technique. Even if linear boundary conditions are used, the iterative technique is necessary because the position of the vortex wake is a very important factor affecting the wave deformation and it can only be found iteratively. Divergence of the iterative technique was observed in three following cases:

- Wave breaking
- Very long computational domain (about 50 chords)
- Froude number is less than 0.8

The method for modeling the free surface was successfully tested by comparisons with measurements for various hydrofoils (see Kornev and Taranov (1998)).

4.2 Calculation of the planing hull

The calculation of the hull is done by assuming planing conditions. This makes the method valid for the upper end of the transition phase and higher as given in Figure 2. The planing hull moving in the vortex wave wake of the front foil is based on the wing analogy discovered by Wagner (1932). Each lifting surface is represented via a set of thin cambered longitudinal strips with rectilinear leading and trailing edges. Such an approximation allows one to model planing surfaces and hydrofoils with curved leading edges, including warped hulls with variable deadrise. If the wetted area of the planing surface is known, the pressure distribution and forces are obtained by using the conventional Vortex Lattice Method (VLM).
A special technique, which in its idea is very similar to the simplified method described by Zhao and Faltinsen (1996) and Mei et al. (1999) for two dimensions, is applied to estimate the wetted area of a three dimensional planing surface with an arbitrary length to beam ratio. This method is rather simple and can be written in a general form that covers complex planing geometry moving in the vortex-wave wake. The essential points of this approach are described shortly below.

Consider a longitudinal strip of a planing surface (see Fig.5). The wetted chords of strip are calculated iteratively. In the first iteration, the wetted chord is determined as a length measured from the trailing edge to the point of intersection between bottom contour and the free surface either not disturbed or disturbed by the front foil. The free surface deformation caused by the planing surface itself can be written in the n-th iteration in the form of the streamline equation

$$y^n = y(-\infty) + \int_{-\infty}^{x_0^n} v_y^n(\xi)/(V_\infty + v_x^n(\xi))d\xi \qquad (8)$$

where v_x and v_y are components of velocity induced by the entire planing surface and hydrofoil in the n-th iteration. They can be obtained by using the Biot-Savart law. In the iterations the leading edge x_o^n is shifted towards the positive direction of the x-axis by adding Δ_x along the bottom contour until the intersection point between the streamline Eq. (14) and the bottom contour (i.e. the critical point) will be lay within the chord $x_0<x_{int}<x_1$. Performing calculations for all sides and strips and connecting corresponding points one obtains the wetted area of the planing surface. Obviously, the jet flow near the leading edge and sides of the planing hull is neglected in this

approach. It should also be noted that the integral Eq. (8) converges only in the three-dimensional case.

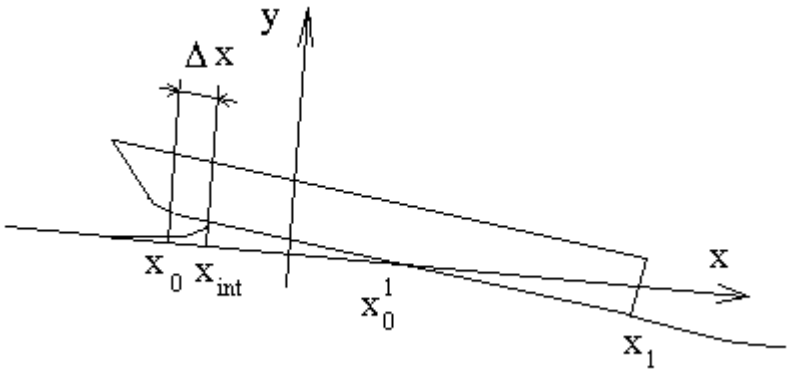

Figure 5: Vortex Lattice of the free surface and vortex wake behind the hydrofoil

5. Influence of the free surface deformation on the hydrodynamic forces of the catamaran

One of the peculiarities of the present theory is consideration of the free surface deformation. The front foil disturbs the free surface, producing a wave whose length is proportional to the Froude number. A reasonable question is whether the free surface deformation plays a significant role and whether it is possible to neglect the free surface effects saving the computational time and simplifying the design process. Fig. 6 below allows one to answer this question.

The results indicated as "w/o deformation" were obtained without consideration of the free surface deformation. Both the planing hull and the front foil move on and under the undisturbed free surface. As seen from the figures, the theoretical results obtained with account for the free surface deformation converge to measurements when the Froude number is increased. On the contrary, a neglect of the free surface effects, leads to a large discrepancy between measurements and the numerical prediction. The reason is clear. The larger the Froude number the longer the wave after the front foil. The wave trough reaches the planing hull and, therefore, the influence of the free surface deformation becomes larger.

6. Optimization of Hydrofoil Assisted Catamarans

The developed method was used for the investigation of hydrodynamics of a Hysuwac type Hydrofoil assisted catamaran with particulars as given in Table 1. The investigation was directed at finding the optimal way to retrofit existing catamarans with hydrofoils. Focus was therefore on investigating different foils and the mutual position of the foils and the hull, while not changing the hull geometry.

The numerical calculations showed that among the geometric parameters investigated, the most effective tool to optimize the catamaran is the lateral distance between the foils. The effect of other parameters was comparable with the accuracy of the numerical approach. The calculation included both the determination of the hydrodynamic forces and attitude of the ship.

Figure 8 and 9 display results. Three different cases, schematically sketched in the Fig.7, are considered. Firstly, the basic variant of the Hysuwac arrangement (Case 1), secondly, the same arrangement but with the rear foil shifted towards aft by 3 m (Case 2). Finally, the arrangement of the Hysuwac with hull and the rear foil shifted aft by 7 meters with respect to the front foil or, in other words, the front foil shifted forward towards the bow by 7 m (Case 3). A clear tendency emerged: that increasing the distance between foils results in an improvement of the L/D ratio.

The results presented in the Fig.8 were obtained without considering wave resistance. As seen in the figure, the best case is the Case 2, followed by Case 3 and then the Case 1.

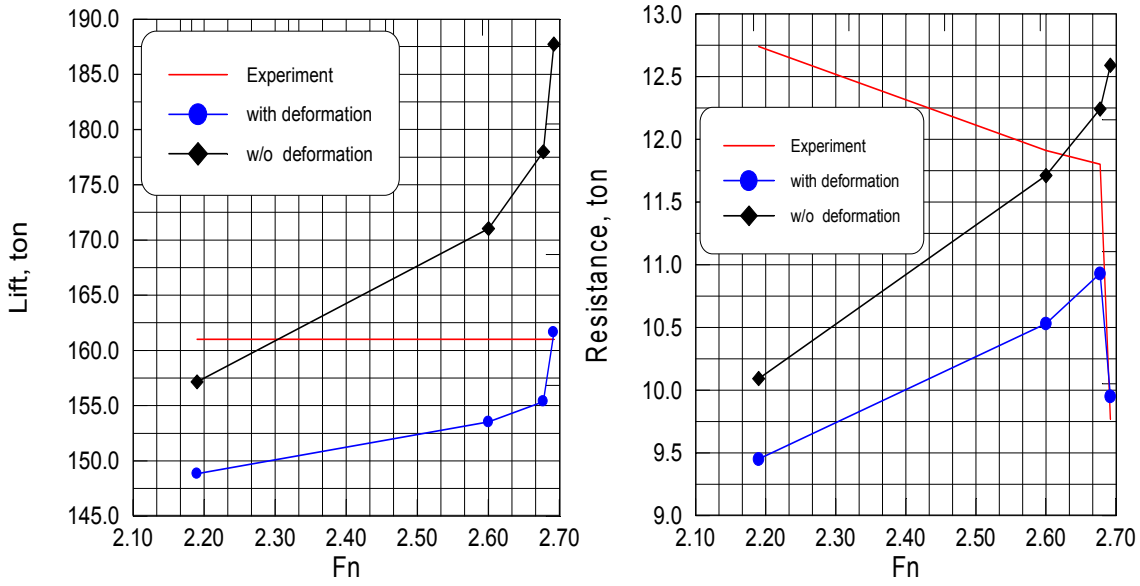

Figure 6: Lift and resistance versus the Froude number Fn.

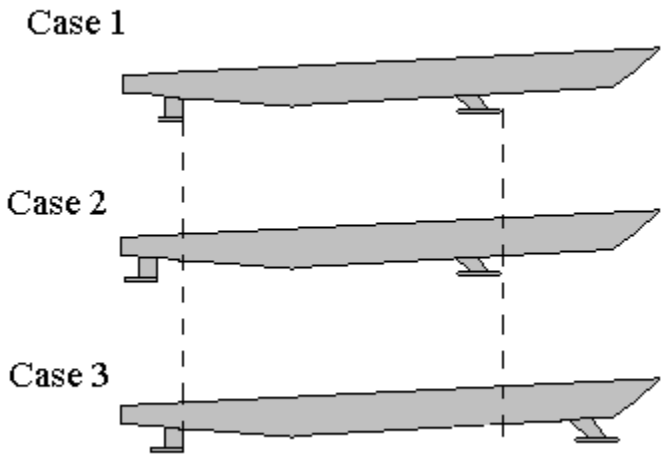

Figure 7: Schematic sketches of the arrangement in three cases

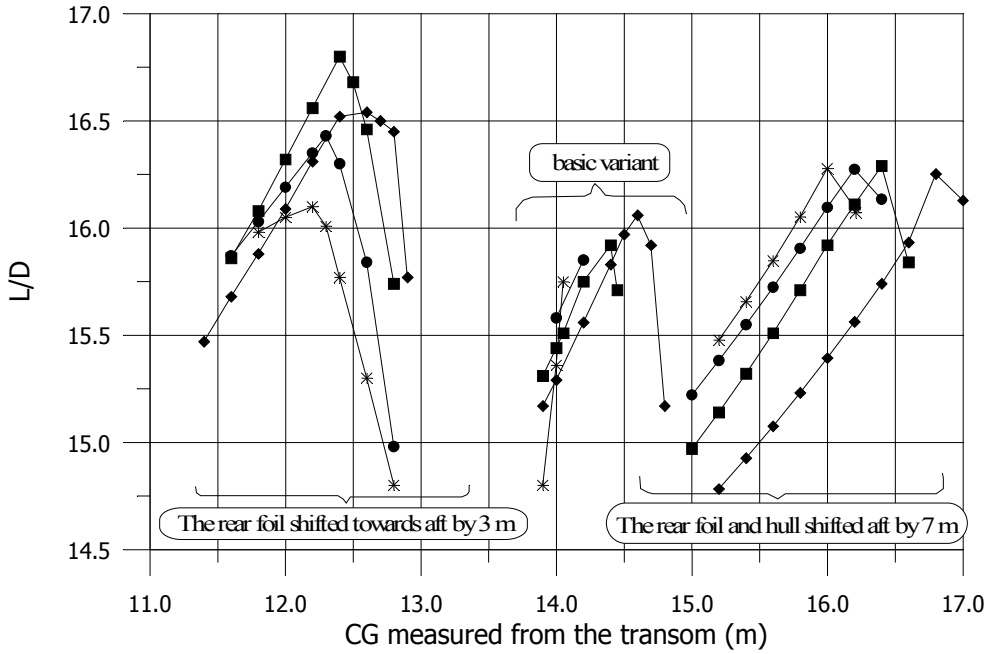

Figure 8: The L/D ratio versus the position of the center of gravity for three cases . The wave resistance is not taken into account. Diamonds- 170 t, bars- 180 t, circles- 190 t, stars- 200 t

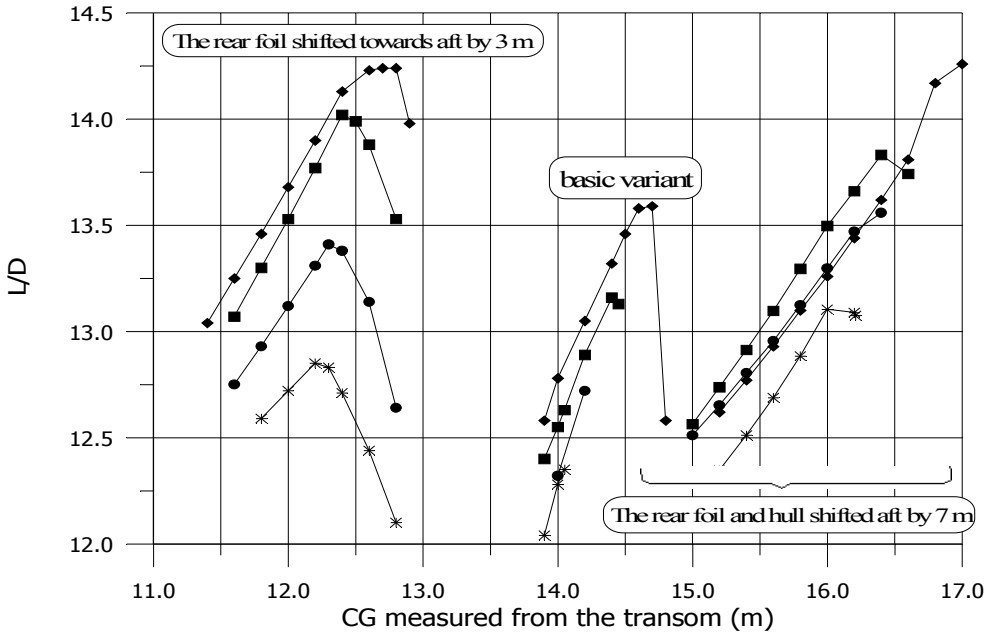

Figure 9: The L/D ratio versus the position of the center of gravity for three cases . The wave resistance is taken into account. Diamonds- 170 t, bars- 180 t, circles- 190 t, stars- 200 t

To explain this result, consider the Table 2 and Figures 10-12 illustrating the three results obtained for the center of gravity position at the point securing the best L/D ratio for given weight: 170 ton at a speed of 40 knots. Table 2 gives the results for Cases 2 and 3 as percentage values of Case 1, which is considered to be 100%.

Table 2: Calculated results for Cases 2 and 3 in relation to Case 1

	Basic variant	The rear foil is shifted by 3 m towards aft	Both the rear foil and the hull are shifted by 7 m towards aft
	Case 1	Case 2	Case 3
Pitch angle	2.147°	2.079°	1.652°
Submergence	-0.476 m	-0.54 m	-0.704 m
Lift coeff. of the front foil	100 %	83.1 %	92.5 %
L/D of the front foil	100 %	98.6 %	63.8 %
Lift coeff of the rear foil	100 %	106 %	107.4 %
L/D of the rear foil	100 %	107 %	136.9 %
Lift coeff. of the hull+ the rear foil	100 %	102 %	103.5 %
L/D of the system Planning hull+rear foil	100 %	109 %	101.8 %
Wave Resistance ton	100 %	87 %	79.8 %
L/D of the ship	100 %	105 %	104.3 %

As seen from the Fig.12, the larger the distance, between the front foil and the rear foil, the larger the up wash induced by waves. The reason is clear. In the first case the rear foil is located close to the wave trough. The foil located behind the wave trough utilizes the positive up wash induced by waves (see Fig.11). That is why the lift coefficients of the rear foil and the rear lifting system (the rear foil+hull) are the maximal for Case 3 (see Table 2). The L/D ratio of the rear foil is also maximal for Case 3. Because the lift and the L/D ratio are increased when we shift the rear foil aft, the L/D ratio is larger for Cases 2 and 3 than for Case 1.
The increase in lift of the rear lifting system leads to the ship rising further out of the water (see Table 2). The wetted area is decreased being minimal for Case 2 (see Fig.10). The increase of lift leads to a decrease of the pitch angle and consequently the lift of the front foil (see Table 2). Therefore, the intensity of the tip vortex shed from the front foil is also decreased, weakening the downwash induced by the tip vortex on the rear foil (see Fig.12). Again, it leads to an increase of the lift on the rear lifting system. Despite of the fact that the lift decreases with decreasing pitch angle, the lift of the rear lifting system becomes larger. The two effects increasing the lift (i.e. less downwash induced by the weaker tip vortex and increased up wash induced by wave crest) prove to be stronger effects.

Because the wetted area is maximal in Case 3, this arrangement has the largest fraction of the hull friction resistance. This is why the L/D ratio of Case 3 is less than that of Case 2. However, the positive influence of shifting the front foil forward resulting in higher lift for the rear lifting system proves to be sufficient to improve the L/D ratio of Case 3 compared to that of Case 1. Accounting for the wave resistance (see Fig. 9) makes the results for the Cases 2 and 3 closer. The wave resistance was calculated using Michel's theory as implemented in the program Michlet 6.06 developed by Dr.Lazauskas (2000). The wave induced by the front foil is not considered in this approach. Comparison of computed results with experiments for the basic variant showed that the overall resistance prediction is within 5% of measured values.

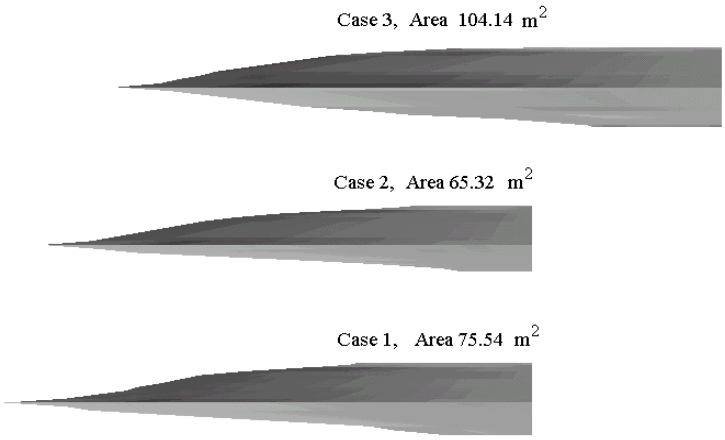

Figure 10: Wetted area of the catamaran hull for three cases.

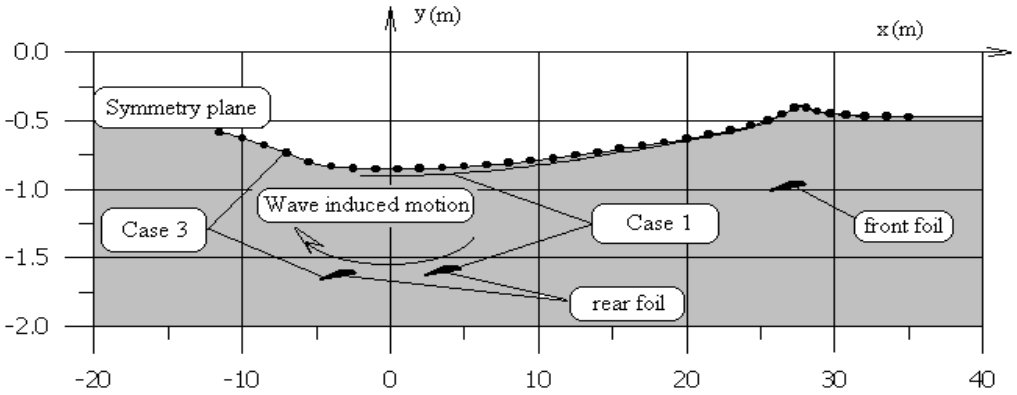

Figure 11: The mutual positions of the rear foil and the wave surface at 40 knots.

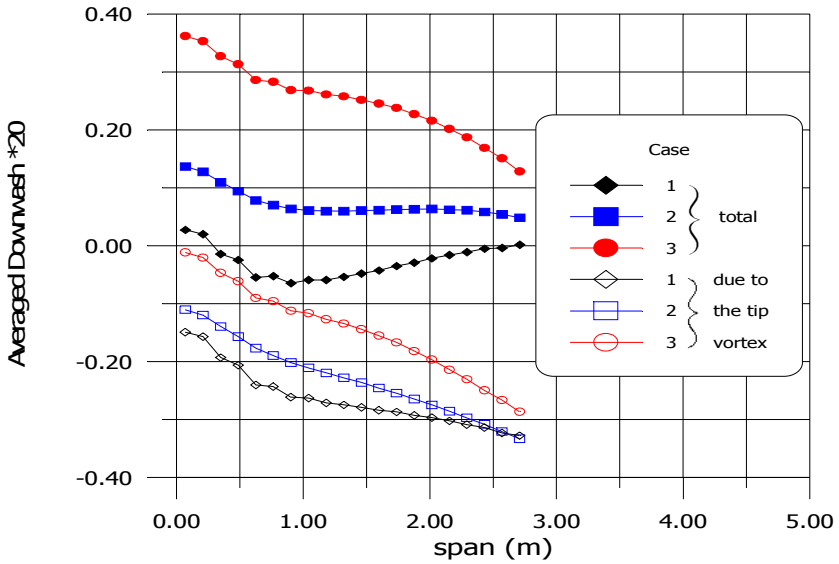

Figure 12: The downwash (up wash if positive) averaged along the chord B.

The first tendency observed by shifting only the rear foil aft in Case 2 was clearly confirmed in the tests performed at the University of Stellenbosch. The second tendency found in Case 3 (shifting the front foil towards bow) is rather an unexpected one because, as a rule, an increase in wetted area of that magnitude leads to an overall increase in resistance. Therefore, the result presented here, is material for discussion and needs further experimental investigations.

7. Conclusions and future work

The main hydrodynamic design principles of hydrofoil-assisted catamarans have been presented, and existing designs reviewed. The importance of the interactions between the foils and hull are illustrated through calculations with the proposed mathematical model. The mathematical model provides an effective basis for design of hydrofoil-assisted catamarans. The method was thoroughly tested for the Hysuwac design based on model test results. The model has no restrictive factors, typical for instance for the slender hull theory and other approaches, and can be generalized for small Froude numbers accounting for the gravity effects.

A technical measure for optimization, following from this purely numerical investigation would be to increase the distance between the rear foil and the front foil so that it the rear lifting system benefits from the up wash of the front foil. Experimental tendencies validate the result. Further experimental investigations will be conducted to investigate variations in foil placements for the Hysuwac system. This data will be used to validate and extend the theoretical method into a versatile design tool for hydrofoil-assisted catamarans.

References

HOERNER, S. (1965), *Fluid Dynamic Drag*, Published by Author, Bricktown, New Jersey.

HOPPE, K.G. (1992), *Boat, Hydrofoil supported Catamarans*, S.A. Patent No. 82/3505 and Foreign Patents.

HOPPE, K.G. (1991), *Performance Evaluation of High Speed Surface Craft with Reference to the Hysucat Development*, Fast Ferry International, Vol. 30(No.s 1 & 3), Jan. & Apr.

HOPPE, K.G. (1995), *Optimization of Hydrofoil Supported Planing Catamarans,* FAST'95, Third International Conference on Fast Sea Transportation, pp. 307-317.

HOPPE, K.G. (1998), *S.A. Patent App. 98/3763* and *U.S. Patent No. 6,.164,235 of 26/12/2000*.

HOPPE, K.G. (1999), *Hydrofoil Catamaran Developments in South Africa*, HIPER'99, First International Conference on High Performance Marine Vehicles, Zewenwacht, South Africa.

HOPPE, K.G.; MIGEOTTE, G. (2000), *Model Tests on the Voyager II Foil Assisted Catamaran*, ITM Report, Dept. of Mech. Engineering, University of Stellenbosch. Not available to the public.

JORDE, J.H. (1991), *The Development of a 50 knots, 40m FoilCat*, IMAS'91 High Speed Marine Transportation Conference, pp. 79-84.

KORNEV, N.V. (1998), *The Computational Method of Vortex Elements and its Application to Hydro-Aerodynamics*, 2nd Doctor Thesis, Marine Tech. Univ. of St. Petersburg, Dept. of Hydromechanics. In Russian.

KORNEV, N.V.; TARANOV, A., (1998), *Investigation of the Vortex-Wave Wake behind a Hydrofoil*, Ship Technology Research 46, pp. 8-13.

LAZAUSKAS, L., (2000), *Michlet 6.06*, freeware on the Internet: www.maths.adelaide.edu.au/Applied/llazausk/hydro/hydro.htm

MEI, X.; LUI, Y.; YUE, D.K.P. (1999), *On the Water Impact of General Two-Dimensional Sections*, Applied Ocean Research 21, pp 1-15.

MIGEOTTE, G.; HOPPE, K.G. (1999), *Development of hydrofoil Assisted Catamarans with Semi-Displacement Hulls*, FAST'99, Fifth International Conference on Fast Sea Transportation, pp. 631-642.

MIYATA, H., (1989), *Development of a New Type Hydrofoil Catamaran*, J. of Ship Res. 33 (2).

SAVITSKY, D. (1964), *Hydrodynamic Design of Planing Hulls,* Marine Technology, October, pp. 71-95.

SHIMIZU, K.; MASUYAMA, K.; YAGI, H. (1994), *Hydrodynamic Design Philosophies of the Hybrid Hydrofoil Catamaran*, Techno-Ocean'94 Proceedings, pp. 265-270.

TAO, M. (1998), *Development of the Foil Augmented Wave Piercing Catamaran*, RINA International Conference of Fast Freight Transportation by Sea.

TAO, M. (2000), *Resistance Prediction Method of Foil Augmented Cat*, HPMV2000, Third International Conference on High Performance Marine Vehicles, pp. 172—176.

THIART, G. (1997), *Vortex Lattice Method for a Straight Hydrofoil near a Free Surface*, International Shipbuilding Progress, 44 (5), pp. 5-26.

WAGNER, H. (1932), *Űber Stoss-und Gleitvorgänge an der Wasseroberfläche von Flüsigkeiten*, Z. Angew. Math. Mech. 12(4), pp. 193-215.

ZHAO, R.; FALTINSEN, O.; AARSNES, J. (1996), *Water Entry of Two-Dimensional Sections with and Without Flow Separation*, Proceedings 21st Symposium on Naval Hydrodynamics.